EURASIP Journal on Applied Signal Processing 2004:5, 649–661

Performance Comparisons of MIMO Techniques with Application to WCDMA Systems

Chuxiang Li
Department of Electrical Engineering, Columbia University, New York, NY 10027, USA
Email: cxli@ee.columbia.edu

Xiaodong Wang
Department of Electrical Engineering, Columbia University, New York, NY 10027, USA
Email: wangx@ee.columbia.edu

Received 11 December 2002; Revised 1 August 2003

Multiple-input multiple-output (MIMO) communication techniques have received great attention and gained significant development in recent years. In this paper, we analyze and compare the performances of different MIMO techniques. In particular, we compare the performance of three MIMO methods, namely, BLAST, STBC, and linear precoding/decoding. We provide both an analytical performance analysis in terms of the average receiver SNR and simulation results in terms of the BER. Moreover, the applications of MIMO techniques in WCDMA systems are also considered in this study. Specifically, a subspace tracking algorithm and a quantized feedback scheme are introduced into the system to simplify implementation of the beamforming scheme. It is seen that the BLAST scheme can achieve the best performance in the high data rate transmission scenario; the beamforming scheme has better performance than the STBC strategies in the diversity transmission scenario; and the beamforming scheme can be effectively realized in WCDMA systems employing the subspace tracking and the quantized feedback approach.

Keywords and phrases: BLAST, space-time block coding, linear precoding/decoding, subspace tracking, WCDMA.

1. INTRODUCTION

Multiple-input multiple-output (MIMO) communication technology has received significant recent attention due to the rapid development of high-speed broadband wireless communication systems employing multiple transmit and receive antennas [1, 2, 3]. Many MIMO techniques have been proposed in the literature targeting at different scenarios in wireless communications. The BLAST system is a layered space-time architecture originally proposed by Bell Labs to achieve high data rate wireless transmissions [4, 5, 6]. Note that the BLAST systems do not require the channel knowledge at the transmitter end. On the other hand, for some applications, the channel knowledge is available at the transmitter, at least partially. For example, an estimate of the channel at the receiver can be fed back to the transmitter in both frequency division duplex (FDD) and time division duplex (TDD) systems, or the channel can be estimated directly by the transmitter during its receiving mode in TDD systems. Accordingly, several channel-dependent signal processing schemes have been proposed for such scenarios, for example, linear precoding/decoding [7]. The linear precoding/decoding schemes achieve performance gains by allocating power and/or rate over multiple transmit antennas, with partially or perfectly known channel state information [7]. Another family of MIMO techniques aims at reliable transmissions in terms of achieving the full diversity promised by the multiple transmit and receive antennas. Space-time block coding (STBC) is one of such techniques based on orthogonal design that admits simple linear maximum likelihood (ML) decoding [8, 9, 10]. The trade-off between diversity and multiplexing gain are addressed in [11, 12], which are from a signal processing perspective and from an information theoretic perspective, respectively.

Some simple MIMO techniques have already been proposed to be employed in the third-generation (3G) wireless systems [13, 14]. For example, in the 3GPP WCDMA standard, there are open-loop and closed-loop transmit diversity options [15, 16]. As more powerful MIMO techniques emerge, they will certainly be considered as enabling techniques for future high-speed wireless systems (i.e., 4G and beyond).

The purpose of this paper is to compare the performance of different MIMO techniques for the cases of two and four transmit antennas, which are realistic scenarios for MIMO applications. For a certain transmission rate, we

compare the performance of three MIMO schemes, namely, BLAST, STBC, and linear precoding/decoding. Note that both BLAST and STBC do not require channel knowledge at the transmitter, whereas linear precoding/decoding does. For each of these cases, we provide an analytical performance analysis in terms of the receiver output average signal-to-noise ratio (SNR) as well as simulation results on their BER performance. Moreover, we also consider the application of these MIMO techniques in WCDMA systems with multipath fading channel. In particular, when precoding is used, a subspace tracking algorithm is needed to track the eigenspace of the MIMO system at the receiver and feed back this information to the transmitter [17, 18, 19, 20]. Since the feedback channel typically has a very low bandwidth [21], we contrive an efficient and effective quantized feedback approach.

The main findings of this study are as follows.

(i) In the high data rate transmission scenario, for example, four symbols per transmission over four transmit antennas, the BLAST system actually achieves a better performance than the linear precoding/decoding schemes, even though linear precoding/decoding make use of the channel state information at the transmitter.

(ii) In the diversity transmission scenario, for example, one symbol per transmission over two or four transmit antennas, beamforming offers better performance than the STBC schemes. Hence the channel knowledge at the transmitter helps when there is some degree of freedom to choose the eigen channels.

(iii) By employing the subspace tracking technique with an efficient quantized feedback approach, the beamforming scheme can be effective and feasible to be employed in WCDMA systems to realize reliable data transmissions.

The remainder of this paper is organized as follows. In Section 2, performance analysis and comparisons of different MIMO techniques are given for the narrowband scenario. Section 3 describes the WCDMA system based on the 3GPP standard, the channel estimation method, the algorithm of tracking the MIMO eigen-subspace, as well as the quantized feedback approach. Simulation results and further discussions are given in Section 4. Section 5 contains the conclusions.

2. PERFORMANCE ANALYSIS AND COMPARISONS OF MIMO TECHNIQUES

In this section, we analyze the performance of several MIMO schemes under different transmission rate assumptions, for the cases of two and four transmit antennas. BLAST and linear precoding/decoding schemes are studied and compared for high-rate transmissions in Section 2.1. Section 2.2 focuses on the diversity transmission scenario, where different STBC strategies are investigated and compared with beamforming and some linear precoding/decoding approaches.

2.1. BLAST versus linear precoding for high-rate transmission

Assume that there are n_T transmit and n_R receive antennas, where $n_R \geq n_T$. In this section, we assume that the MIMO system is employed to achieve the highest data rate, that is, n_T symbols per transmission. When the channel is unknown to the transmitter, the BLAST system can be used to achieve this; whereas when the channel is known to the transmitter, the linear precoding/decoding can be used to achieve this.

2.1.1. BLAST

In the BLAST system, at each transmission, n_T data symbols $s_1, s_2, \ldots, s_{n_T}$, $s_i \in \mathcal{A}$, where $\mathcal{A}$ is some unit-energy (i.e., $\mathbb{E}\{|s_i|^2\} = 1$) constellation signal set (e.g., PSK, QAM), are transmitted simultaneously from all n_T antennas. The received signal can be represented by

$$\underbrace{\begin{bmatrix} y_1 \\ y_2 \\ \vdots \\ y_{n_R} \end{bmatrix}}_{\mathbf{y}} = \sqrt{\frac{\rho}{n_T}} \underbrace{\begin{bmatrix} h_{1,1} & h_{1,2} & \cdots & h_{1,n_T} \\ h_{2,1} & h_{2,2} & \cdots & h_{2,n_T} \\ \vdots & \vdots & \ddots & \vdots \\ h_{n_R,1} & h_{n_R,2} & \cdots & h_{n_R,n_T} \end{bmatrix}}_{\mathbf{H}} \underbrace{\begin{bmatrix} s_1 \\ s_2 \\ \vdots \\ s_{n_T} \end{bmatrix}}_{\mathbf{s}} + \underbrace{\begin{bmatrix} n_1 \\ n_2 \\ \vdots \\ n_{n_R} \end{bmatrix}}_{\mathbf{n}}, \tag{1}$$

where y_i denotes the received signal at the ith receive antenna; $h_{i,j}$ denotes the complex channel gain between the ith receive antenna and the jth transmit antenna; ρ denotes the total transmit SNR; and $\mathbf{n} \sim \mathcal{N}_c(\mathbf{0}, \mathbf{I}_{n_R})$.

The received signal is first matched filtered to obtain $\mathbf{z} = \mathbf{H}^H\mathbf{y} = \sqrt{\rho/n_T}\mathbf{H}^H\mathbf{H}\mathbf{s} + \mathbf{H}^H\mathbf{n}$. Denote $\mathbf{\Omega} \triangleq \mathbf{H}^H\mathbf{H}$ and $\mathbf{w} \triangleq \mathbf{H}^H\mathbf{n}$, and thus, $\mathbf{w} \sim \mathcal{N}_c(\mathbf{0}, \mathbf{\Omega})$. The matched-filter output is then whitened to get

$$\mathbf{u} = \mathbf{\Omega}^{-1/2}\mathbf{z} = \sqrt{\frac{\rho}{n_T}}\mathbf{\Omega}^{1/2}\mathbf{s} + \tilde{\mathbf{v}}, \tag{2}$$

where $\tilde{\mathbf{v}} \triangleq \mathbf{\Omega}^{-1/2}\mathbf{w} \sim \mathcal{N}_c(\mathbf{0}, \mathbf{I}_{n_R})$. Based on (2), several methods can be used to detect the symbol vector $\mathbf{s}$. For example, the ML detection rule is given by

$$\hat{\mathbf{s}}_{\mathrm{ML}} = \arg\min_{\mathbf{s} \in \mathcal{A}^{n_T}} \left\| \mathbf{u} - \sqrt{\frac{\rho}{n_T}}\mathbf{\Omega}^{1/2}\mathbf{s} \right\|^2, \tag{3}$$

which has a computational complexity exponential in the number of transmit antennas n_T. On the other hand, the sphere decoding algorithm offers a near-optimal solution to (2) with an expected complexity of $\mathcal{O}(n_T^3)$ [22]. Moreover, a linear detector makes a symbol-by-symbol decision $\hat{\mathbf{s}} = \mathbb{Q}(\mathbf{x})$, where $\mathbf{x} = \mathbf{G}\mathbf{u}$ and $\mathbb{Q}(\cdot)$ denotes the symbol slicing operation. Two forms of linear detectors can be used [5, 6], namely, the linear zero-forcing detector, where $\mathbf{G} = \mathbf{\Omega}^{-1/2}$, and the linear MMSE detector, where $\mathbf{G} = (\mathbf{\Omega}^{1/2} + (n_T/\rho)\mathbf{I})^{-1}$. Finally, a method based on interference cancellation with ordering offers improved performance over the linear detectors with comparable complexity [22]. Note that among

the above-mentioned BLAST decoding algorithms, the linear zero-forcing detector has the worst performance. The decision statistics of this method is given by

$$\mathbf{x} = \mathbf{G}\mathbf{u} = \mathbf{\Omega}^{-1/2}\mathbf{u} = \sqrt{\frac{\rho}{n_T}}\mathbf{s} + \mathbf{\Omega}^{-1/2}\tilde{\mathbf{v}}. \tag{4}$$

It follows from (4) that the received SNR for symbol s_j is $(\rho/n_T)/[\mathbf{\Omega}^{-1}]_{j,j}$, $j = 1, 2, \ldots, n_T$. Hence the average received SNR under linear zero-forcing BLAST detection is given by

$$\overline{\mathrm{SNR}}_{\text{BLAST-LZF}} = \rho\left(\frac{1}{n_T^2}\sum_{j=1}^{n_T}\frac{1}{[\mathbf{\Omega}^{-1}]_{j,j}}\right). \tag{5}$$

2.1.2. Linear precoding and decoding

When the channel $\mathbf{H}$ is known to the transmitter, a linear precoder can be employed at the transmitter and a corresponding linear decoder can be used at the receiver [7]. Specifically, suppose $m \le n_T$ symbols $\mathbf{s} = [s_1 \;\; s_2 \;\; \cdots \;\; s_m]^T$ are transmitted per transmission, where $m = \mathrm{rank}(\mathbf{H})$. Then the linear precoder is an $n_T \times m$ matrix $\mathbf{F}$ such that the transmitted signal is $\mathbf{Fs}$. The $n_R \times 1$ received signal vector is then

$$\mathbf{y} = \mathbf{HFs} + \mathbf{n}, \tag{6}$$

where $\mathbf{n} \sim \mathcal{N}_c(\mathbf{0}, \mathbf{I}_{n_R})$. At the receiver, $\mathbf{y}$ is first matched filtered, and then an $m \times n_T$ linear decoder $\mathbf{G}$ is applied to the matched-filter output to obtain the decision statistics

$$\mathbf{x} = \mathbf{GH}^H\mathbf{y} = \mathbf{G\Omega Fs} + \mathbf{GH}^H\mathbf{n}. \tag{7}$$

The linear precoder $\mathbf{F}$ and decoder $\mathbf{G}$ are chosen to minimize a weighted combination of symbol estimation errors, that is, $\min_{\mathbf{F},\mathbf{G}} \mathbb{E}\{\|\mathbf{D}^{1/2}(\mathbf{s}-\mathbf{x})\|^2\}$, where $\mathbf{D}$ is a diagonal positive definite matrix subject to the total transmitter power constraint $\mathrm{tr}(\mathbf{FF}^H) \le \rho$. The weight matrix $\mathbf{D}$ is such that all decoded symbols have equal errors (equal error design). Denote the eigendecomposition of $\mathbf{\Omega}$ as $\mathbf{\Omega} = \mathbf{V\Lambda V}^H + \tilde{\mathbf{V}}\tilde{\mathbf{\Lambda}}\tilde{\mathbf{V}}^H$, where $\mathbf{\Lambda}$ and $\mathbf{V}$ contain the m largest eigenvalues and the corresponding eigenvectors of $\mathbf{\Omega}$, respectively; and $\tilde{\mathbf{\Lambda}}$ and $\tilde{\mathbf{V}}$ contain the remaining $(n_T - m)$ eigenvalues and the corresponding eigenvectors, respectively. Denote $\gamma = \rho/\mathrm{tr}(\mathbf{\Lambda}^{-1})$. Then the linear precoder and decoder are given by [7]

$$\begin{aligned}\mathbf{F} &= \gamma^{1/2}\mathbf{V\Lambda}^{-1/2},\\ \mathbf{G} &= \frac{1}{\gamma^{-1/2} + \gamma^{1/2}}\mathbf{\Lambda}^{-1/2}\mathbf{V}^H.\end{aligned} \tag{8}$$

It can be verified that $\mathbf{GH}^H\mathbf{HF} = (1/(\gamma^{-1} + \gamma))\mathbf{I}_m$. Hence this precoding scheme transforms the MIMO channel into a scaled identity matrix. Furthermore, the received SNRs for all decoded symbols are equal, given by γ, that is,

$$\overline{\mathrm{SNR}}_{\text{equal-error precoding}} = \frac{\rho}{\mathrm{tr}\,(\mathbf{\Lambda}^{-1})} = \frac{\rho}{\mathrm{tr}\,(\mathbf{\Omega}^{-1})}. \tag{9}$$

Remark 1. The BLAST system can be viewed as a special case of linear precoding with the transmitter filter $\mathbf{F} = \sqrt{\rho/n_T}\mathbf{I}_{n_T}$. And the zero-forcing BLAST detection scheme corresponds to choosing the receiver filter $\mathbf{G} = \mathbf{\Omega}^{1/2}$.

Remark 2. An alternative precoding scheme is to choose $\mathbf{F} = \sqrt{\rho/n_T}\mathbf{V}$ and $\mathbf{G} = \mathbf{V}^H$. Then the output of the linear decoder can be written as

$$\mathbf{x} = \sqrt{\frac{\rho}{n_T}}\mathbf{V}^H\mathbf{H}^H\mathbf{HVs} + \mathbf{V}^H\mathbf{H}^H\mathbf{n} = \sqrt{\frac{\rho}{n_T}}\mathbf{\Lambda}\boldsymbol{s} + \mathbf{w}, \tag{10}$$

where $\mathbf{w} \sim \mathcal{N}_c(\mathbf{0}, \mathbf{\Lambda})$. Hence this scheme also transforms the MIMO channel into a set of independent channels, but with different SNRs. The received SNR for the jth symbol is $(\rho/n_T)\lambda_j$, where λ_j is the jth eigenvalue contained by $\mathbf{\Lambda}$. We call this method the whitening precoding. The average received SNR is given by

$$\overline{\mathrm{SNR}}_{\text{whitening precoding}} = \rho\left(\frac{1}{n_T^2}\sum_{j=1}^{n_T}\lambda_j\right) = \rho\left(\frac{\mathrm{tr}(\mathbf{\Omega})}{n_T^2}\right). \tag{11}$$

Note that the whitening precoding is different from the equal-error precoding in (8). In particular, different received SNRs are achieved over different subchannels for the whitening precoding, whereas the equal-error precoding provides the same SNR over all subchannels.

2.1.3. Comparisons

We have the following result on the relative SNR performance of the BLAST system and the two precoding schemes discussed above.

Proposition 1. *Suppose that an $n_T \times n_R$ MIMO system is employed to transmit n_T symbols per transmission, using either the BLAST system, the equal-error precoding scheme, or the whitening precoding scheme, then*

$$\begin{aligned}\overline{\mathrm{SNR}}_{\text{whitening precoding}} &\ge \overline{\mathrm{SNR}}_{\text{BLAST-LZF}}\\ &\ge \overline{\mathrm{SNR}}_{\text{equal-error precoding}}.\end{aligned} \tag{12}$$

Proof. We first show that

$$\overline{\mathrm{SNR}}_{\text{BLAST-LZF}} \ge \overline{\mathrm{SNR}}_{\text{equal-error precoding}}. \tag{13}$$

Since

$$\frac{1}{n_T}\sum_{j=1}^{n_T}\lambda_j^{-1} = \frac{1}{n_T}\sum_{j=1}^{n_T}[\mathbf{\Omega}^{-1}]_{j,j} \ge \frac{n_T}{\sum_{j=1}^{n_T}(1/[\mathbf{\Omega}^{-1}]_{j,j})}, \tag{14}$$

we have

$$\frac{1}{n_T^2}\sum_{j=1}^{n_T}\frac{1}{[\mathbf{\Omega}^{-1}]_{j,j}} \ge \frac{1}{\sum_{j=1}^{n_T}\lambda_j^{-1}}. \tag{15}$$

It follows from (5), (9), and (15) that $\overline{\mathrm{SNR}}_{\text{BLAST-LZF}} \ge \overline{\mathrm{SNR}}_{\text{equal-error precoding}}$.

We next show that $\overline{\text{SNR}}_{\text{BLAST-LZF}} \leq \overline{\text{SNR}}_{\text{whitening precoding}}$. First, we have the following.

Fact 1. Suppose that $\mathbf{A}$ is a $n \times n$ positive definite matrix, then

$$\frac{1}{[\mathbf{A}^{-1}]_{i,i}} = A_{i,i} - \tilde{\mathbf{a}}_i^H \tilde{\mathbf{A}}_i^{-1} \tilde{\mathbf{a}}_i, \tag{16}$$

where $\tilde{\mathbf{A}}_i$ is the $(n-1) \times (n-1)$ matrix obtained from $\mathbf{A}$ by removing the ith row and ith column; and $\tilde{\mathbf{a}}_i$ is the ith column of $\mathbf{A}$ with the ith entry $A_{i,i}$ removed. Note that $\tilde{\mathbf{A}}_i$ is a principal submatrix of $\mathbf{A}$; since $\mathbf{A}$ is positive definite, so is, $\tilde{\mathbf{A}}_i$, and $\tilde{\mathbf{A}}_i^{-1}$ exists. To see (16), denote the above-mentioned partitioning of the Hermitian matrix $\mathbf{A}$ with respect to the ith column and row by $\mathbf{A} = (\tilde{\mathbf{A}}_i, \tilde{\mathbf{a}}_i, A_{i,i})$. In the same way, we partition its inverse $\mathbf{B} \triangleq \mathbf{A}^{-1} = (\tilde{\mathbf{B}}_i, \tilde{\mathbf{b}}_i, B_{i,i})$. Now from the fact that $\mathbf{AB} = \mathbf{I}_n$, it follows that

$$A_{i,i}B_{i,i} + \tilde{\mathbf{a}}_i^H \tilde{\mathbf{b}}_i = 1, \qquad \tilde{\mathbf{a}}_i B_{i,i} + \tilde{\mathbf{A}}_i \tilde{\mathbf{b}}_i = \mathbf{0}. \tag{17}$$

Solving for $B_{i,i}$ from (17), we obtain (16).

Using (16), we have

$$\sum_{j=1}^{n_T} \frac{1}{[\mathbf{\Omega}^{-1}]_{j,j}} = \sum_{j=1}^{n_T} \left(\Omega_{i,i} - \tilde{\boldsymbol{\omega}}_i^H \tilde{\mathbf{\Omega}}_i^{-1} \tilde{\boldsymbol{\omega}}_i\right) \leq \sum_{j=1}^{n_T} \Omega_{i,i} = \text{tr}(\mathbf{\Omega}). \tag{18}$$

It then follows from (5), (11), and (18) that $\overline{\text{SNR}}_{\text{BLAST-LZF}} \leq \overline{\text{SNR}}_{\text{whitening precoding}}$. □

Figure 1 shows the comparisons between the BLAST and the linear precoding/decoding schemes in terms of the average receiver SNR as well as the BER for a system with $n_T = 4$ and $n_R = 6$. The rate is four symbols per transmission. The SNR curves in Figure 1a are plotted according to (9), (5), and (11). It is seen that the SNR curves confirm the conclusion of Proposition 1. Moreover, it is interesting to see that the SNR ordering given by (12) does not translate into the corresponding BER order. This can be roughly explained as follows. The BER for the ith symbol stream can be approximated as $Q(\gamma\sqrt{\text{SNR}_i})$, where γ is a constant determined by the modulation scheme. The average BER is then

$$\overline{p} \cong \frac{1}{n_T} \sum_{i=1}^{n_T} Q\left(\gamma\sqrt{\text{SNR}_i}\right). \tag{19}$$

Since $Q(\cdot)$ is a concave function, we have

$$\overline{p} \leq Q\left(\gamma\sqrt{\overline{\text{SNR}}}\right). \tag{20}$$

Hence, the average SNR value does not directly translate into the average BER. Moreover, it is seen from the Figure 1b in Figure 1 that the interference cancellation with ordering [6] BLAST detection method offers a significant performance gain over the linear zero-forcing method, making the BLAST outperform the precoding schemes by a substantial margin.

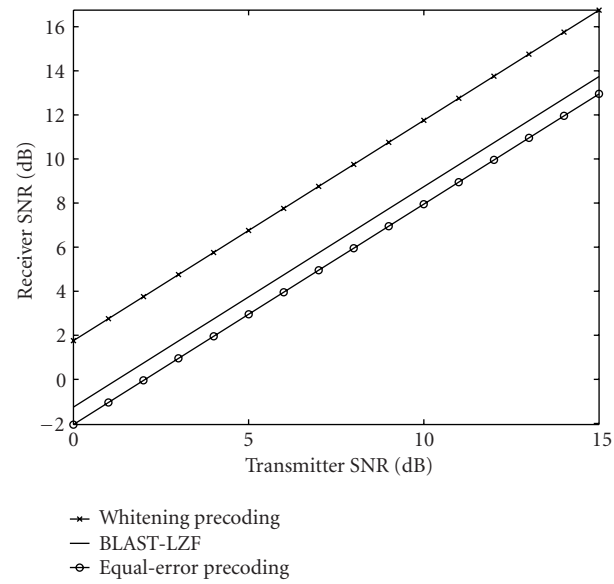

(a)

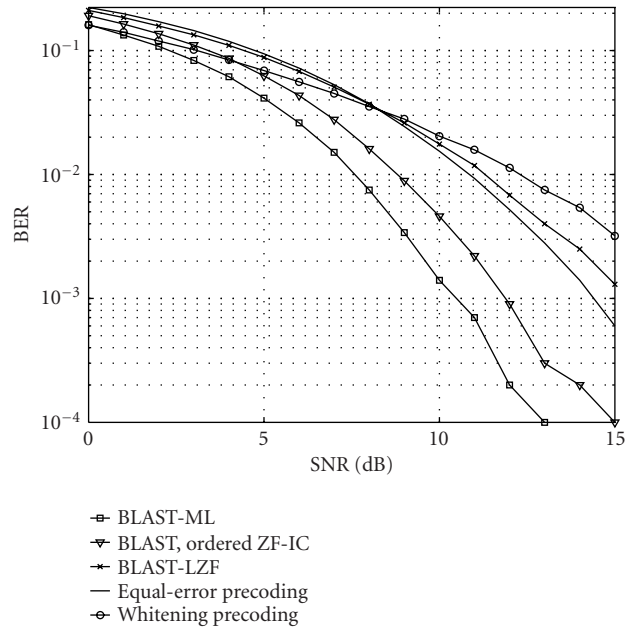

(b)

Figure 1: Comparisons of the average receiver SNR and the BER between the BLAST and the linear precoding/decoding schemes: $n_T = 4$ and $n_R = 6$; the rate is four symbols/transmission.

2.2. Space-time block coding versus beamforming for diversity transmission

In contrast to the high data rate MIMO transmission scenario discussed in Section 2.1, an alternative approach to exploiting MIMO systems targets at achieving the full diversity. For example, with n_T transmit antennas and n_R receive

antennas, a maximum diversity order of $n_T n_R$ is possible when the transmission rate is one symbol per transmission. When the channel is unknown at the transmitter, this can be achieved using STBC (for $n_T = 2$); and when the channel is known at the transmitter, this can be achieved using beamforming.

2.2.1. Two transmit antennas case

Alamouti scheme

When $n_T = 2$, the elegant Alamouti transmission scheme can be used to achieve full diversity transmission at one symbol per transmission [8]. It transmits two symbols s_1 and s_2 over two consecutive transmissions as follows. During the first transmission, s_1 and s_2 are transmitted simultaneously from antennas 1 and 2, respectively; during the second transmission, $-s_2^*$ and s_1^* are transmitted simultaneously from transmit antennas 1 and 2, respectively. The received signals at receive antenna i corresponding to these two transmissions are given by

$$\begin{bmatrix} y_i(1) \\ y_i(2) \end{bmatrix} = \sqrt{\frac{\rho}{2}} \begin{bmatrix} s_1 & s_2 \\ -s_2^* & s_1^* \end{bmatrix} \begin{bmatrix} h_{i,1} \\ h_{i,2} \end{bmatrix} + \begin{bmatrix} n_i(1) \\ n_i(2) \end{bmatrix}, \quad i = 1, 2, \ldots, n_R. \tag{21}$$

Note that (21) can be rewritten as follows:

$$\underbrace{\begin{bmatrix} y_i(1) \\ y_i(2)^* \end{bmatrix}}_{\mathbf{y}_i} = \sqrt{\frac{\rho}{2}} \underbrace{\begin{bmatrix} h_{i,1} & h_{i,2} \\ h_{i,2}^* & -h_{i,1}^* \end{bmatrix}}_{\tilde{\mathbf{H}}_i} \underbrace{\begin{bmatrix} s_1 \\ s_2 \end{bmatrix}}_{\mathbf{s}} + \underbrace{\begin{bmatrix} n_i(1) \\ n_i(2)^* \end{bmatrix}}_{\mathbf{n}_i}, \quad i = 1, 2, \ldots, n_R, \tag{22}$$

where $\mathbf{n}_i \overset{\text{i.i.d.}}{\sim} \mathcal{N}_c(\mathbf{0}, \mathbf{I}_2)$. Note that the channel matrix $\tilde{\mathbf{H}}_i$ is orthogonal, that is, $\tilde{\mathbf{H}}_i^H \tilde{\mathbf{H}}_i = (|h_{i,1}|^2 + |h_{i,2}|^2)\mathbf{I}_2$.

At each receive antenna, the received signal is matched filtered to obtain

$$\mathbf{z}_i = \tilde{\mathbf{H}}_i^H \mathbf{y}_i = \sqrt{\frac{\rho}{2}} \left(|h_{i,1}|^2 + |h_{i,2}|^2 \right) \mathbf{s} + \mathbf{w}_i, \quad i = 1, 2, \ldots, n_R, \tag{23}$$

where $\mathbf{w}_i \sim \mathcal{N}_c(\mathbf{0}, (|h_{i,1}|^2 + |h_{i,2}|^2)\mathbf{I}_2)$. The final decision on $\mathbf{s}$ is then made according to $\hat{\mathbf{s}} = \mathbb{Q}(\mathbf{z})$, where $\mathbb{Q}(\cdot)$ denotes the symbol slicing operation, and

$$\mathbf{z} = \sum_{i=1}^{n_R} \mathbf{z}_i = \sqrt{\frac{\rho}{2}} \left[\sum_{i=1}^{n_R} \left(|h_{i,1}|^2 + |h_{i,2}|^2 \right) \right] \mathbf{s} + \sum_{i=1}^{n_R} \mathbf{w}_i. \tag{24}$$

The received SNR is therefore given by

$$\begin{aligned} \text{SNR}_{\text{Alamouti}} &= \frac{(\rho/2)\left[\sum_{i=1}^{n_R} \left(|h_{i,1}|^2 + |h_{i,2}|^2 \right) \right]^2}{\sum_{i=1}^{n_R} \left(|h_{i,1}|^2 + |h_{i,2}|^2 \right)} \\ &= \frac{\rho}{2} \operatorname{tr}(\mathbf{H}_A^H \mathbf{H}_A) = \frac{\rho}{2} \operatorname{tr}(\mathbf{\Omega}_A) = \rho \left(\frac{\lambda_1 + \lambda_2}{2} \right), \end{aligned} \tag{25}$$

where $\mathbf{\Omega}_A \triangleq \mathbf{H}_A^H \mathbf{H}_A$, λ_1 and λ_2 are the two eigenvalues of $\mathbf{\Omega}_A$, and

$$\mathbf{H}_A = \begin{bmatrix} h_{1,1} & h_{1,2} \\ h_{2,1} & h_{2,2} \\ \vdots & \vdots \\ h_{n_R,1} & h_{n_R,2} \end{bmatrix}, \qquad \mathbf{\Omega}_A = \mathbf{H}_A^H \mathbf{H}_A. \tag{26}$$

Beamforming

Beamforming can be referred to as maximum ratio weighting [23], and it is a special case of the linear precoding/decoding discussed in Section 2.1.2, where

$$\begin{aligned} \mathbf{F} &= \sqrt{\rho}\mathbf{v}_1, \\ \mathbf{G} &= \mathbf{v}_1^H, \end{aligned} \tag{27}$$

and $\mathbf{v}_1$ is the eigenvector corresponding to the largest eigenvalue of $\mathbf{\Omega}$. Hence in the beamforming scheme, at each transmission, the transmitter transmits $\mathbf{v}_1 s$ from all transmit antennas, where s is a data symbol. The received signal is given by

$$\mathbf{y} = \mathbf{H}\mathbf{F}s + \mathbf{n} = \sqrt{\rho}\mathbf{H}\mathbf{v}_1 s + \mathbf{n}. \tag{28}$$

At the receiver, a decision on s is made according to $\hat{s} = \mathbb{Q}(u)$, where the decision statistic u is given by $u = \mathbf{v}_1^H \mathbf{H}^H \mathbf{y} = \sqrt{\rho} \underbrace{\mathbf{v}_1^H \mathbf{\Omega} \mathbf{v}_1}_{\lambda_1} s + \underbrace{\mathbf{v}_1^H \mathbf{H}^H \mathbf{n}}_{\mathcal{N}_c(0,\lambda_1)}$. The received SNR in this case is

$$\text{SNR}_{\text{beamforming}} = \rho\lambda_1. \tag{29}$$

Comparing (25) with (29), it is obvious that $\text{SNR}_{\text{beamforming}} \geq \text{SNR}_{\text{Alamouti}}$. Note that in this case, the SNR order indeed translates into the BER order; since in the Alamouti scheme, both symbols have the same SNR, then

$$p_{\text{beamforming}} = Q\left(\gamma\sqrt{\rho\lambda_1} \right) \leq Q\left(\gamma\sqrt{\frac{\rho}{2}(\lambda_1 + \lambda_2)} \right) = p_{\text{Alamouti}}. \tag{30}$$

2.2.2. Four transmit antennas case

One symbol per transmission

It is known that rate-one orthogonal STBC only exists for $n_T = 2$, that is, the Alamouti code. For the case of four transmit antennas ($n_T = 4$), we adopt a rate-one (almost orthogonal) transmission scheme with the following transmission matrix:

$$\mathbf{S} = \begin{bmatrix} s_1 & s_2 & s_3 & s_4 \\ s_2^* & -s_1^* & s_4^* & -s_3^* \\ s_3 & -s_4 & -s_1 & s_2 \\ s_4^* & s_3^* & -s_2^* & -s_1^* \end{bmatrix}. \tag{31}$$

Such a transmission scheme was proposed in [24]. Hence four symbols s_1, s_2, s_3, and s_4 are transmitted across four transmit antennas over four transmissions. The received signals at the ith receive antenna corresponding to these four

transmissions are given by

$$\begin{bmatrix} y_i(1) \\ y_i(2) \\ y_i(3) \\ y_i(4) \end{bmatrix} = \sqrt{\frac{\rho}{4}}\mathbf{S}\begin{bmatrix} h_{i,1} \\ h_{i,2} \\ h_{i,3} \\ h_{i,4} \end{bmatrix} + \begin{bmatrix} n_i(1) \\ n_i(2) \\ n_i(3) \\ n_i(4) \end{bmatrix}, \quad i = 1, 2, \ldots, n_R. \tag{32}$$

Note that (32) can be rewritten as

$$\underbrace{\begin{bmatrix} y_i(1) \\ y_i(2)^* \\ y_i(3) \\ y_i(4)^* \end{bmatrix}}_{\mathbf{y}_i} = \sqrt{\frac{\rho}{4}}\underbrace{\begin{bmatrix} h_{i,1} & h_{i,2} & h_{i,3} & h_{i,4} \\ -h_{i,2}^* & h_{i,1}^* & -h_{i,4}^* & h_{i,3}^* \\ -h_{i,3} & h_{i,4} & h_{i,1} & -h_{i,2} \\ -h_{i,4}^* & -h_{i,3}^* & h_{i,2}^* & h_{i,1}^* \end{bmatrix}}_{\tilde{\mathbf{H}}_i}\underbrace{\begin{bmatrix} s_1 \\ s_2 \\ s_3 \\ s_4 \end{bmatrix}}_{\mathbf{s}} + \underbrace{\begin{bmatrix} n_i(1) \\ n_i(2)^* \\ n_i(3) \\ n_i(4)^* \end{bmatrix}}_{\mathbf{v}_i}, \quad i = 1, 2, \ldots, n_R. \tag{33}$$

The matched-filter output at the ith receive antenna is given by

$$\mathbf{z}_i = \tilde{\mathbf{H}}_i^H \mathbf{y}_i = \sqrt{\frac{\rho}{4}}\tilde{\mathbf{\Omega}}_i \mathbf{s} + \mathbf{w}_i, \tag{34}$$

where

$$\tilde{\mathbf{\Omega}}_i = \tilde{\mathbf{H}}_i^H \tilde{\mathbf{H}}_i = \begin{bmatrix} \gamma_i & 0 & \alpha_i & 0 \\ 0 & \gamma_i & 0 & -\alpha_i \\ -\alpha_i & 0 & \gamma_i & 0 \\ 0 & \alpha_i & 0 & \gamma_i \end{bmatrix}, \tag{35}$$

$\gamma_i = \sum_{j=1}^{n_T} |h_{i,j}|^2$, $\alpha_i = 2\jmath\Im(h_{i,1}^* h_{i,3} + h_{i,4}^* h_{i,2})$, and $\mathbf{w}_i = \tilde{\mathbf{H}}_i^H \mathbf{n}_i \sim \mathcal{N}_c(\mathbf{0}, \tilde{\mathbf{\Omega}}_i)$. By grouping the entries of $\mathbf{z}_i$ into two pairs, we can write

$$\begin{aligned} \underbrace{\begin{bmatrix} z_i(1) \\ z_i(3) \end{bmatrix}}_{\mathbf{z}_{i,1}} &= \sqrt{\frac{\rho}{4}}\mathbf{\Gamma}_i \underbrace{\begin{bmatrix} s_1 \\ s_3 \end{bmatrix}}_{\mathbf{s}_1} + \underbrace{\begin{bmatrix} w_i(1) \\ w_i(3) \end{bmatrix}}_{\mathbf{w}_{i,1}}, \\ \underbrace{\begin{bmatrix} z_i(4) \\ z_i(2) \end{bmatrix}}_{\mathbf{z}_{i,2}} &= \sqrt{\frac{\rho}{4}}\mathbf{\Gamma}_i \underbrace{\begin{bmatrix} s_4 \\ s_2 \end{bmatrix}}_{\mathbf{s}_2} + \underbrace{\begin{bmatrix} w_i(4) \\ w_i(2) \end{bmatrix}}_{\mathbf{w}_{i,2}}, \end{aligned} \tag{36}$$

where $\mathbf{\Gamma}_i = \begin{bmatrix} \gamma_i & \alpha_i \\ -\alpha_i & \gamma_i \end{bmatrix}$ and $\mathbf{w}_{i,\ell} \sim \mathcal{N}_c(\mathbf{0}, \mathbf{\Gamma}_i)$, $\ell = 1, 2$. Note that $\mathbf{\Gamma}_i^H = \mathbf{\Gamma}_i$. Note also that (36) are effectively 2×2 BLAST systems and they can be decoded using either linear detection or ML detection. For example, the linear decision rule is given by $\hat{\mathbf{s}}_\ell = \mathbb{Q}[\sum_{i=1}^{n_R} \mathbf{G}_{i,\ell}\mathbf{z}_{i,\ell}]$, $\ell = 1, 2$, where the linear detector can be either a zero-forcing detector, that is, $\mathbf{G}_{i,\ell} = \mathbf{\Gamma}_i^{-1}$, or an MMSE detector, that is, $\mathbf{G}_{i,\ell} = (\mathbf{\Gamma}_i + (4/\rho)\mathbf{I}_2)^{-1}$. On the other hand, the ML detection rule is given by

$$\begin{aligned} \hat{\mathbf{s}}_\ell &= \min_{\mathbf{s}\in\mathcal{A}^2} \sum_{i=1}^{n_R} \left(\mathbf{z}_{i,\ell} - \sqrt{\frac{\rho}{4}}\mathbf{\Gamma}_i\mathbf{s}\right)^H \mathbf{\Gamma}_i^{-1}\left(\mathbf{z}_{i,\ell} - \sqrt{\frac{\rho}{4}}\mathbf{\Gamma}_i\mathbf{s}\right) \\ &= \max_{\mathbf{s}\in\mathcal{A}^2} \left[\Re\left\{\mathbf{s}^H \sum_{i=1}^{n_R} \mathbf{z}_{i,\ell}\right\} - \sqrt{\frac{\rho}{4}}\mathbf{s}^H\left(\sum_{i=1}^{n_R}\mathbf{\Gamma}_i\right)\mathbf{s}\right], \quad \ell = 1, 2. \end{aligned} \tag{37}$$

When the channel state is known at the transmitter, the optimal transmission method to achieve one symbol per transmission is the beamforming scheme described by (27), (28), and (29).

Note that the received SNR of the above block coding scheme with linear zero-forcing detector is given by

$$\overline{\mathrm{SNR}} = \frac{\rho}{4} \cdot \frac{n_R^2}{\sum_{i=1}^{n_R} [\mathbf{\Gamma}_i^{-1}]_{1,1}}, \tag{38}$$

whereas the SNR of the beamforming scheme is given by $\overline{\mathrm{SNR}}_{\text{beamforming}} = \rho\lambda_1$.

Two symbols per transmission

Now suppose that a rate of two symbols per transmission is desired using four transmit antennas. When the channel is unknown at the transmitter, we can use one pair of the transmit antennas to transmit $\mathbf{s}_1 = [s_1 \;\; s_2]^T$ using the Alamouti scheme, and use the other pair to transmit $\mathbf{s}_2 = [s_3 \;\; s_4]^T$ also using Alamouti scheme. In this way, we transmit four symbols over two transmissions. At the ith receive antenna, the received signal $\mathbf{y}_i = [y_i(1) \;\; y_i(2)]^T$ corresponding to the two transmissions is given by

$$\mathbf{y}_i = \sqrt{\frac{\rho}{2}}\tilde{\mathbf{H}}_{i,1}\mathbf{s}_1 + \sqrt{\frac{\rho}{2}}\tilde{\mathbf{H}}_{i,2}\mathbf{s}_2, +\mathbf{n}, \quad i = 1, 2, \ldots, n_R, \tag{39}$$

where $\tilde{\mathbf{H}}_{i,1} = \begin{bmatrix} h_{i,1} & h_{i,2} \\ h_{i,2}^* & -h_{i,1}^* \end{bmatrix}$ and $\tilde{\mathbf{H}}_{i,2} = \begin{bmatrix} h_{i,3} & h_{i,4} \\ h_{i,4}^* & -h_{i,3}^* \end{bmatrix}$. Therefore, we have

$$\underbrace{\begin{bmatrix} \mathbf{y}_1 \\ \mathbf{y}_2 \\ \vdots \\ \mathbf{y}_{n_R} \end{bmatrix}}_{\mathbf{y}} = \sqrt{\frac{\rho}{2}}\underbrace{\begin{bmatrix} \tilde{\mathbf{H}}_{1,1} & \tilde{\mathbf{H}}_{1,2} \\ \tilde{\mathbf{H}}_{2,1} & \tilde{\mathbf{H}}_{2,2} \\ \vdots & \vdots \\ \tilde{\mathbf{H}}_{n_R,1} & \tilde{\mathbf{H}}_{n_R,2} \end{bmatrix}}_{\tilde{\mathbf{H}}}\underbrace{\begin{bmatrix} s_1 \\ s_2 \\ s_3 \\ s_4 \end{bmatrix}}_{\mathbf{s}} + \mathbf{n}. \tag{40}$$

The received signal $\mathbf{y}$ is first matched filtered to obtain

$$\mathbf{z} = \tilde{\mathbf{H}}^H\mathbf{y} = \sqrt{\frac{\rho}{2}}\tilde{\mathbf{H}}^H\tilde{\mathbf{H}}\mathbf{s} + \tilde{\mathbf{H}}^H\mathbf{n}. \tag{41}$$

Denote

$$\tilde{\mathbf{\Omega}} \triangleq \tilde{\mathbf{H}}^H\tilde{\mathbf{H}} = n_R \cdot \begin{bmatrix} \mathbf{I}_2 & \dfrac{1}{n_R}\displaystyle\sum_{j=1}^{n_R} \tilde{\mathbf{H}}_{j,1}^H\tilde{\mathbf{H}}_{j,2} \\ \dfrac{1}{n_R}\displaystyle\sum_{j=1}^{n_R} \tilde{\mathbf{H}}_{j,1}^H\tilde{\mathbf{H}}_{j,2} & \mathbf{I}_2 \end{bmatrix}. \tag{42}$$

Then the output of the whitening filter is given by $\mathbf{u} = \tilde{\mathbf{\Omega}}^{-1/2}\mathbf{z} = \sqrt{\rho/2}\tilde{\mathbf{\Omega}}^{1/2}\mathbf{s} + \mathbf{w}$, where $\mathbf{w} \sim \mathcal{N}_c(\mathbf{0}, \mathbf{I}_4)$. Now we can use any of the aforementioned BLAST decoding methods to decode $\mathbf{s}$.

When the channel is known at the transmitter, linear precoding/decoding can be used to transmit two symbols per transmission. For example, the equal-error precoding scheme is specified by (8) and (9) with $m = 2$. The received SNR of this method is given by $\overline{\mathrm{SNR}}_{\text{equal-error precoding}} =$

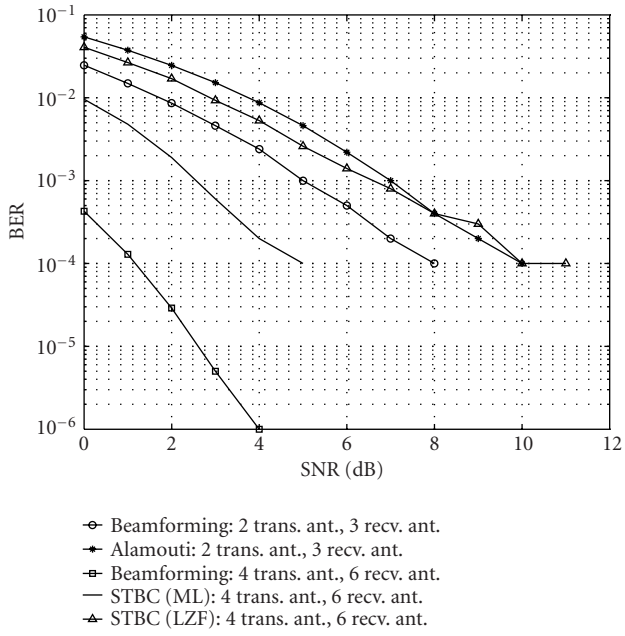

Figure 2: Comparisons of the BER performances among the MIMO techniques for one symbol/transmission: beamforming versus Alamouti with $n_T = 2$ and $n_R = 3$; beamforming versus rate-one STBC with $n_T = 4$ and $n_R = 6$.

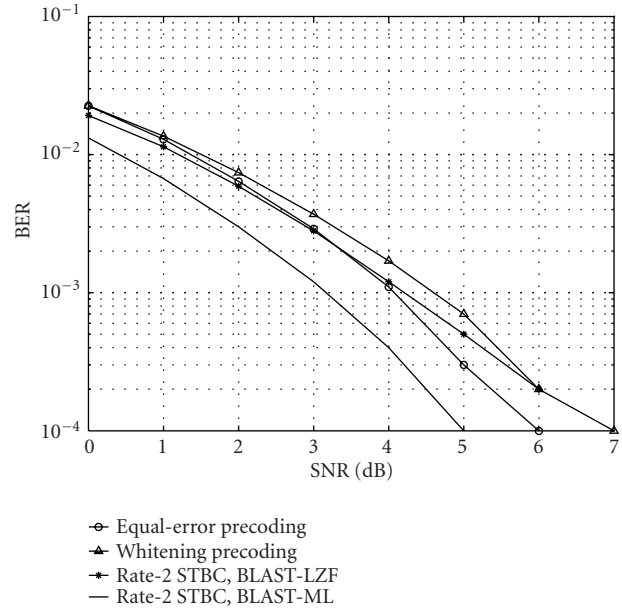

Figure 3: Comparisons of the BER performances between the linear precoding/decoding strategies and the rate-two STBC: $n_T = 4$ and $n_R = 6$; the rate is two symbols/transmission.

$\rho/(\lambda_1^{-1} + \lambda_2^{-1})$. The whitening precoding method, on the other hand, is specified by $\mathbf{F} = \sqrt{\rho/2}[\mathbf{v}_1\mathbf{v}_2]$ and $\mathbf{G} = [\mathbf{v}_1\mathbf{v}_2]^H$; and the average received SNR of this method is given by $\overline{\text{SNR}}_{\text{whitening precoding}} = \rho((\lambda_1 + \lambda_2)/4)$. Note that λ_1 and λ_2 are the two largest eigenvalues contained in $\mathbf{\Lambda}$.

2.2.3. Comparisons

Figure 2 shows the performance comparisons among the MIMO techniques to achieve one symbol per transmission. Specifically, the beamforming scheme is compared with the Alamouti code for a system with two transmit antennas, and the beamforming scheme is compared with the rate-one STBC for a system with four transmit antennas. It is observed from Figure 2 that the beamforming scheme achieves about 2 dB gain over the Alamouti code, and similarly, the beamforming can achieve much better performance than the rate-one STBC strategy.

Figure 3 shows the performance comparisons between the linear precoding/decoding schemes and the rate-two STBC strategy for a system with $n_T = 4$ and $n_R = 6$ to achieve two symbols per transmission. It is seen from Figure 3 that the rate-two STBC achieves a better performance than the linear precoding/decoding schemes, and the performance gap is not so large. In particular, the rate-two STBC with BLAST-LZF decoding has an approximate performance to the equal-error precoding scheme.

It is observed from Figures 1 and 3 that although the linear precoding/decoding schemes exploit the channel knowledge at the transmitter, they may not have performance gains compared to those MIMO techniques without channel knowledge requirement at the transmitter. And this phenomenon is evident especially in the high-data rate transmission scenario, that is, BLAST versus linear precoding/decoding schemes with $n_T = 4$. This can be explained as follows. Note that, for the linear precoding/decoding strategies discussed above, the adaptive modulation is not employed, and thus, the performance gain is limited for the fixed modulation.

3. WCDMA DOWNLINK SYSTEMS

In this section, a WCDMA downlink system based on the 3GPP standard, a subspace tracking algorithm, as well as a quantized feedback approach are specified. In Section 3.1, we describe the WCDMA system, including the structures of the transmitter and the receiver, the channelization and scrambling codes, the frame structures of the data and the pilot channels, the multipath fading channel model, as well as the channel estimation algorithm. In Section 3.2, we detail the subspace tracking method and the quantized feedback scheme.

3.1. System description

3.1.1. Transmitter and receiver structures

The system model of the downlink WCDMA system is shown in Figure 4. The left part of Figure 4 is the transmitter structure. The data sequences of the users are first spread by unique orthogonal variable spreading factor (OVSF) codes ($C_{ch,SF,1}$, $C_{ch,SF,2}, \ldots$), and then, the spread chip sequences of different users are multiplied by downlink scrambling codes ($C_{cs,1}, C_{cs,2}, \ldots$). After summing up the scrambled data

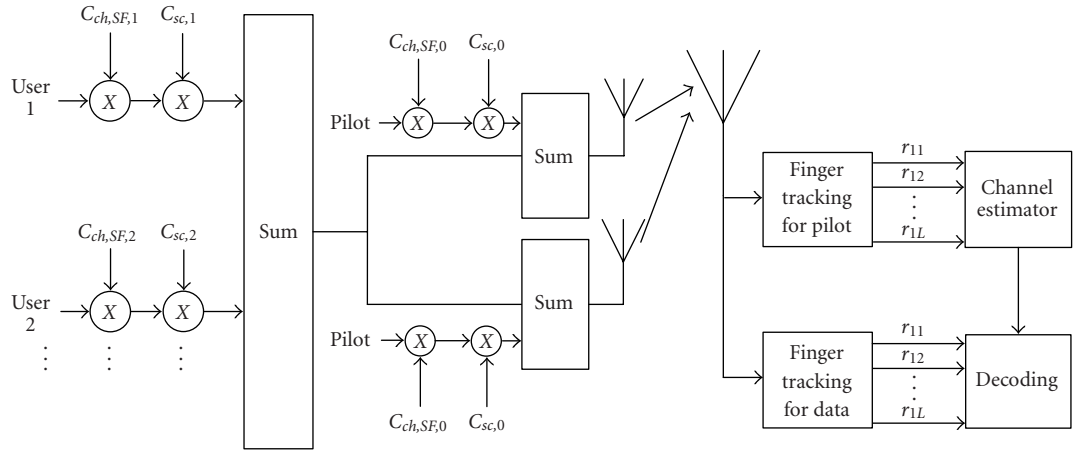

Figure 4: Transmitter and receiver structures of the downlink WCDMA system.

sequences from different users, the data sequences are combined with the pilot sequence, which is also spread and scrambled by the codes $(C_{ch,SF,0}, C_{cs,0})$ for the pilot channel sent to each antenna. The specifications of OVSF and scrambling codes can be referred to [15]. The right part of Figure 4 shows the receiver structure of this system with one receive antenna. We assume the number of multipaths in the WCDMA channel is L. Each receive antenna is followed by a bank of RAKE fingers. Each finger tracks the corresponding multipath component for the receiver antenna and performs descrambling and despreading for each of the L multipath components. Such a receiver structure is similar to the conventional RAKE receiver but without maximal ratio combining (MRC). Hence, there are L outputs for each receive antenna, and thus, each of the L antenna outputs can be viewed as a *virtual* receive antenna [14]. With the received pilot signals, the downlink channel is estimated accordingly. This channel estimate is provided to the detector to perform demodulation of the received users' signals.

It is shown in [14] that the above receiver scheme with *virtual* antennas essentially provides an interface between MIMO techniques and a WCDMA system. The outputs of the RAKE fingers are sent to a MIMO demodulator that operates at the symbol rate. The equivalent symbol-rate MIMO channel response matrix is given by

$$\mathbf{H} = \begin{bmatrix} h_{1,1,1} & h_{1,1,2} & \dots & h_{1,1,n_T} \\ \vdots & \vdots & \ddots & \vdots \\ h_{1,L,1} & h_{1,L,2} & \dots & h_{1,L,n_T} \\ \vdots & \vdots & \ddots & \vdots \\ h_{n_R,1,1} & h_{n_R,1,2} & \dots & h_{n_R,1,n_T} \\ \vdots & \vdots & \ddots & \vdots \\ h_{n_R,L,1} & h_{n_R,L,2} & \dots & h_{n_R,L,n_T} \end{bmatrix}, \tag{43}$$

where $h_{i,l,j}$ denotes the complex channel gain between the jth transmit antenna and the lth finger of the ith receive antenna. Hence (43) is equivalent to a MIMO system with n_T transmit antennas and $(n_R \cdot L)$ receive antennas [14].

3.1.2. Multipath fading channel model and channel estimation

Each user's channel contains four paths, that is, $L = 4$. The channel multipath profile is chosen according to the 3GPP specifications. That is, the relative path delays are 0, 260, 521, and 781 nanoseconds, and the relative path power gains are $0, -3, -6$, and -9 dB, respectively.

There are two channels in the system, namely, common control physical channel (CCPCH) and common pilot channel (CPICH), whose rates are variable and fixed, respectively. For more details, see [15]. The CPICH is transmitted from all antennas using the same channelization and the scrambling code, and the different pilot symbol sequences are adopted on different antennas. Note that in the system, the pilot signal can be treated as the data of a special user. In other words, the pilot and the data of different users in the system are combined with code duplexing but not time duplexing.

Here we use orthogonal training sequences of length $T \geq n_T$ based on the Hadamard matrix to minimize the estimation error [25]. Note that, although the channel varies at the symbol rate, the channel estimator assumes it is fixed over at least n_T symbol intervals.

3.2. Subspace tracking with quantized feedback for beamforming

3.2.1. Tracking of the channel subspace

Recall that in the beamforming and general precoding transmission schemes, the value of the MIMO channel $\mathbf{H}$ has to be provided to the transmitter. Typically, in FDD systems, this can be done by feeding back to the transmitter the estimated channel value $\hat{\mathbf{H}}$. However, the feedback channel usually has a very low data rate. Here we propose to employ a subspace tracking algorithm, namely, projection approximation subspace tracking with deflation (PASTd) [20], with quantized feedback to track the MIMO eigen channels. Figure 5 shows the diagram of the MIMO system adopting a subspace tracking and the quantized feedback approach. In particular, the receiver employs the channel estimator to obtain the estimate of the channel $\hat{\mathbf{H}}$ and subsequently, PASTd algorithm

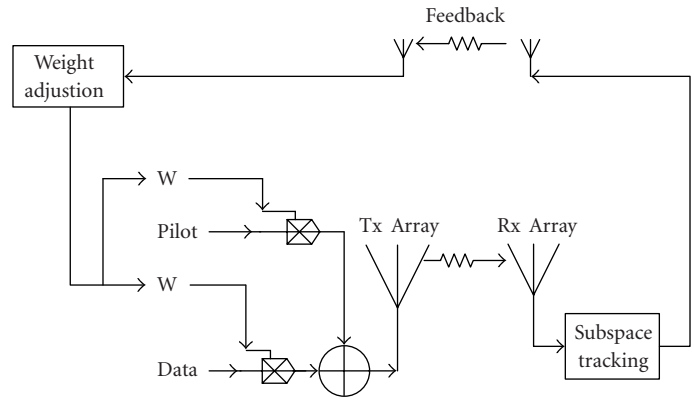

Figure 5: The MIMO linear precoding/decoding system with subspace tracking and quantized feedback schemes.

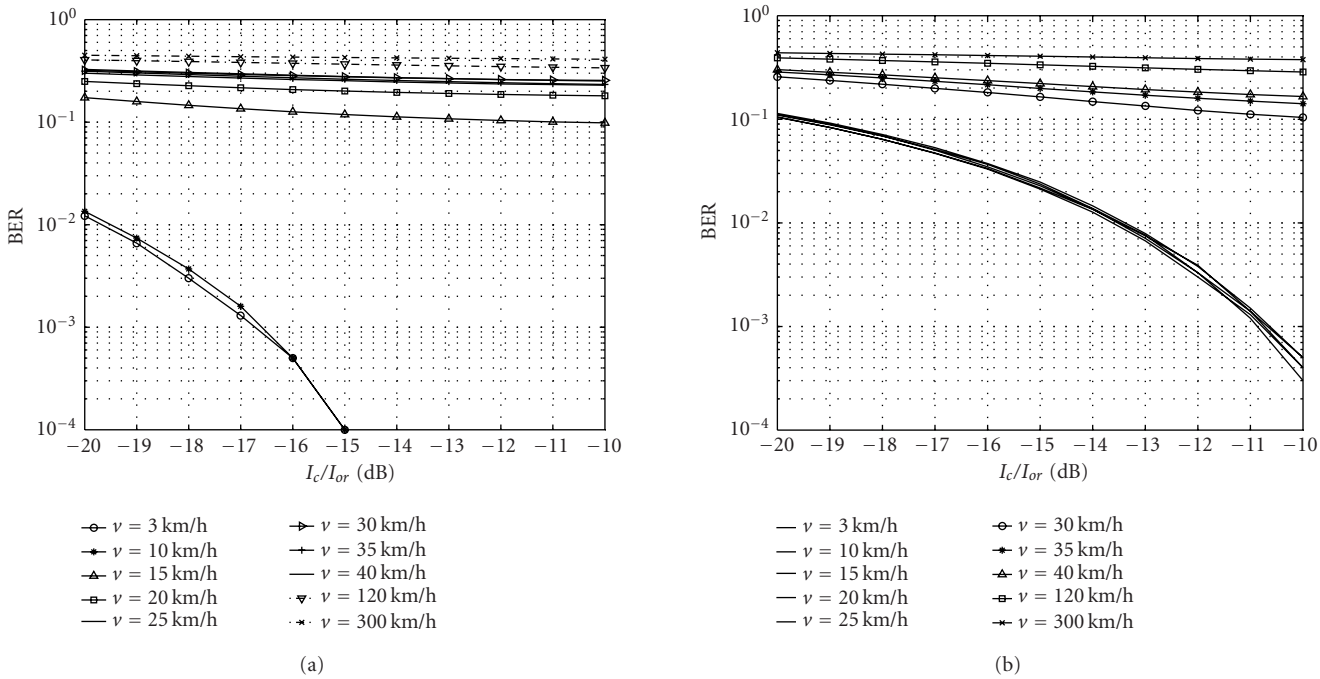

Figure 6: BER performance of beamforming under different doppler frequencies: (a) $n_T = 4$, $n_R = 1$ (beamforming, perfect known channel, lossless feedback (2 frames)), (b) $n_T = 2$, $n_R = 1$ (perfectly known channel, lossless feedback (1 frame)).

is adopted to get $\mathbf{F} = \mathbf{V} = [\mathbf{V}_1, \ldots, \mathbf{V}_m]$, which contains the principal eigenvectors of $\mathbf{\Omega} = \mathbf{H}^H\mathbf{H}$.

3.2.2. Frame-based feedback

Note that, for the uplink channel in the 3GPP standard [21], the bit rate is 1500 bits per second (bps), the frame rate is 100 frames per second (fps), and thus, there are fifteen bits in each uplink frame. On the other hand, the downlink WCDMA channel is a symbol-by-symbol varied channel. Thereby, it is necessary to consider an effective and efficient quantization and feed back scheme, so as to feed back $\mathbf{F}$ to the transmitter via the band-limited uplink channel.

For the beamforming scheme, we employ the feedback approach as follows. The average eigenvector of the channel over one frame or two frames is fed back instead of the eigenvectors of each symbol or slot duration. Note that such feedback approach assumes the downlink WCDMA channel as a block fading one, and actually, it is effective and efficient under low doppler frequencies. Figure 6 shows the BER performances of the MIMO system employing the beamforming scheme under different doppler frequencies. In Figure 6b, two transmit antennas are adopted, and the average eigenvectors over one frame duration are losslessly fed back. That is, the eigenvector information is precisely fed back without

Table 1: Frame structures for quantized feedback. Case 1: two transmit antennas and one receive antenna, (5, 5) quantization : 5 bits for the absolute value component and 5 bits for the phase component of each vector element; A_{ij}: jth bit for the absolute value of ith vector element; P_{ij}: jth bit for the phase of ith vector element. Case 2: two transmit antennas and 1 receive antenna, (4,7) quantization. Case 3: four transmit antennas and 1 receive antenna, (3,6) quantization.

Case 1

Slot	1	2	3	4	5	6	7	8	9	10	11	12	13	14	15
Bits	A_{11}	A_{12}	A_{13}	A_{14}	A_{15}	A_{21}	A_{22}	A_{23}	A_{24}	A_{25}	P_{21}	P_{22}	P_{23}	P_{24}	P_{25}

Case 2

Slot	1	2	3	4	5	6	7	8	9	10	11	12	13	14	15
Bits	A_{11}	A_{12}	A_{13}	A_{14}	A_{21}	A_{22}	A_{23}	A_{24}	P_{21}	P_{22}	P_{23}	P_{24}	P_{25}	P_{26}	P_{27}

Case 3

Slot	1	2	3	4	5	6	7	8	9	10	11	12	13	14	15
Bits	A_{11}	A_{12}	A_{13}	A_{21}	A_{22}	A_{23}	P_{21}	P_{22}	P_{23}	P_{24}	P_{25}	P_{26}	A_{31}	A_{32}	A_{33}
Slot	1	2	3	4	5	6	7	8	9	10	11	12	13	14	15
Bits	P_{31}	P_{32}	P_{33}	P_{34}	P_{35}	P_{36}	A_{41}	A_{42}	A_{43}	P_{41}	P_{42}	P_{43}	P_{44}	P_{45}	P_{46}

quantization. It is seen that the system achieves a good performance for the speeds lower than 30 km/h, and the BER curves are shown as "floors" when v is higher than 30 km/h. The appearance of such "floor" is due to the severe mismatch between the precoding and the downlink channel. Similarly, Figure 6a gives the BER performances of the system employing the beamforming with four transmit antennas, where the average eigenvectors over two frames are losslessly fed back. It is seen that the BER performances degrade to "floors" for the speeds higher than 15 km/h. It is observed from (6) that the frame-based feedback approach is feasible for the beamforming system under the low-speed cases. In particular, it is feasible for the system employing two transmit antennas and four transmit antennas, under the cases of $v \leq 25$ km/h and $v \leq 10$ km/h, respectively.

3.2.3. Quantization of the feedback

Table 1 shows the feedback frame structures for the MIMO system employing beamforming schemes, that is, the quantization of the elements of the eigenvector to be fed back. We consider three cases here. Case 1 and Case 2 are contrived for the beamforming system with two transmit antennas. These two bit allocation strategies of one feedback frame are, namely, (5, 5) and (4, 7) quantized feedback, respectively. In particular, (5, 5) quantized feedback allocates 5 bits each to the absolute value and the phase component of one eigenvector element; and (4, 7) quantized feedback allocates 4 bits and 7 bits to the absolute value and the phase component of one eigenvector element, respectively. Case 3, namely, (3, 6) quantized feedback, is contrived for the beamforming system with four transmit antennas. Two feedback frames are allocated for the average eigenvector over two frames. Note that relatively more bits should be allocated to the phase component, since the error caused by quantization is more sensitive to the preciseness of the phase components than that of the absolute value components moreover, our simulations show that the (5, 5) and (4, 7) quantized feedback approaches actually have very approximated performances.

4. SIMULATION RESULTS FOR WCDMA SYSTEMS

In the simulations, we adopt one receive antenna ($n_R = 1$), which is a realistic scenario for the WCDMA downlink receiver. For the multipath fading channel in the WCDMA system, the number of multipath is assumed to be four ($L = 4$), and the mobile speed is assumed to be three kilometers per hour ($v = 3$ km/h). QPSK is used as the modulation format. The performance metric is BER versus signal-to-interference-ratio (I_c/I_{or}). I_c/I_{or} is the power ratio between the signal of the desired user and the interference from all other simultaneous users in the WCDMA system. Subsequently, several cases with different transmission rates over two and four transmit antennas are studied.

BLAST versus linear precoding

Figure 7 shows the performance comparisons between the BLAST and the linear precoding/decoding schemes for a rate of four symbols per transmission over four transmit antennas ($n_T = 2$). In particular, the channel estimator given in Section 3.1.2 is adopted to acquire the channel knowledge. For the linear precoding/decoding schemes, lossless feedback is assumed. It is seen from Figure 7 that the BLAST scheme with ML detection achieves the best BER performance over all linear precoding/decoding schemes. Note that the reason that precoding does not offer performance advantage here is that we require the rate for different eigen channels to be the same, that is, no adaptive modulation scheme is allowed. Hence we conclude that to achieve high throughput, it suffices to employ the BLAST architecture and the knowledge of the channel at the transmitter offers no advantage.

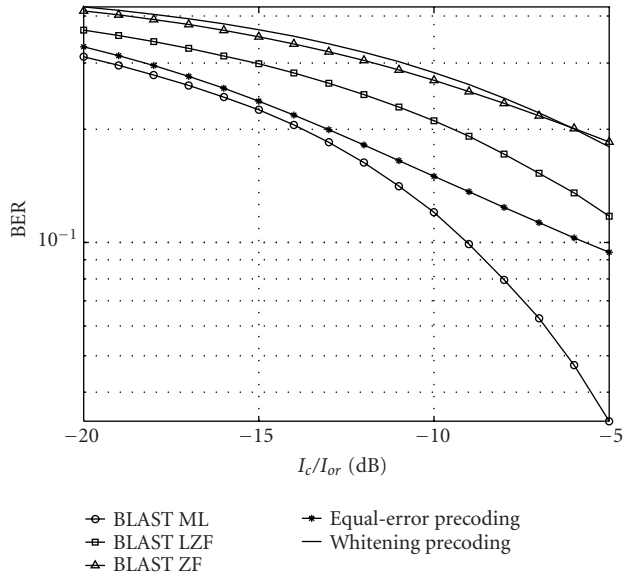

Figure 7: BER comparisons between the BLAST and the transmit precoding schemes: $n_T = 4$ and $n_R = 1$; four QPSK symbols/transmission; $v = 3\,km/h$, $L = 4$.

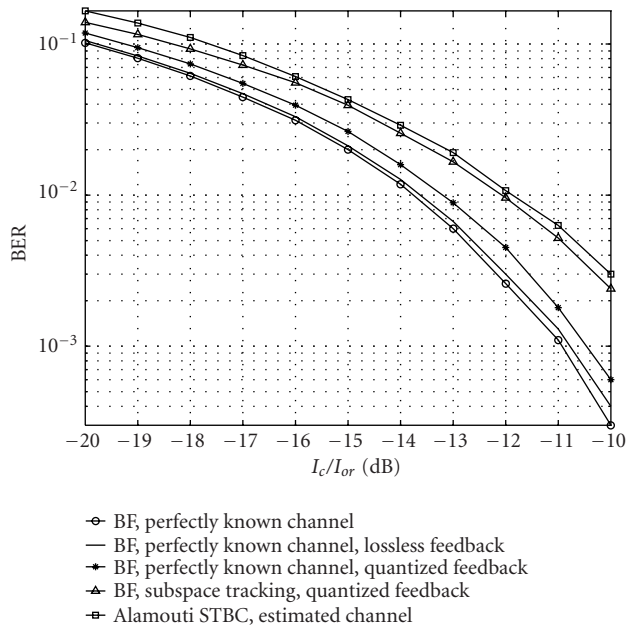

Figure 8: BER comparisons between Alamouti and beamforming with subspace tracking and quantized feedback schemes: $n_T = 2$ and $n_R = 1$; one QPSK symbol/transmission; $v = 3$ km/h; $(4, 7)$ quantized feedback.

STBC versus beamforming

Figure 8 gives the performance comparisons between the Alamouti STBC and the beamforming schemes for a rate of one symbol per transmission over two transmit antennas ($n_T = 2$). The effects of the quantized feedback approach is also shown in Figure 8. In particular, the cycled line is the BER performance when perfect channel knowledge is available at both the transmitter and the receiver. The solid line is the performance when perfect channel knowledge is available at the receiver and the frame-based feedback without quantization in Section 3.2.2 is adopted. It is seen that the frame-based feedback approach only causes very trivial performance degradation. The asteriated line is the performance when perfect channel knowledge is available at the receiver and the frame-based feedback with $(4, 7)$ quantized feedback approach in Section 3.2.3 is adopted. It is seen that the quantization of the feedback only generates about 0.5 dB performance loss. Moreover, the triangled line is the performance when the channel estimator in Section 3.1.2, the subspace tracking in Section 3.2.1, and the $(4, 7)$ quantized feedback approach are adopted. It is shown that the subspace tracking and the channel estimation cause about 1 to 1.5 dB performance degradation. Finally, the squared line is the performance of the Alamouti STBC, where the channel estimator is adopted at the receiver. It is observed from Figure 8 that the WCDMA system employing beamforming can have a better performance than that employing the Alamouti STBC scheme, though the performance gain is not very evident.

Figure 9 gives the comparison between the beamforming scheme and the rate-one STBC strategy discussed in Section 2.2.2 for a rate of one symbol per transmission over four transmit antennas ($n_T = 4$). Similarly, perfectly known channel knowledge, estimated channel knowledge, lossless feedback, and quantized feedback cases are shown. From bottom up, the first curve is the result of the beamforming scheme with perfectly known channel knowledge at both

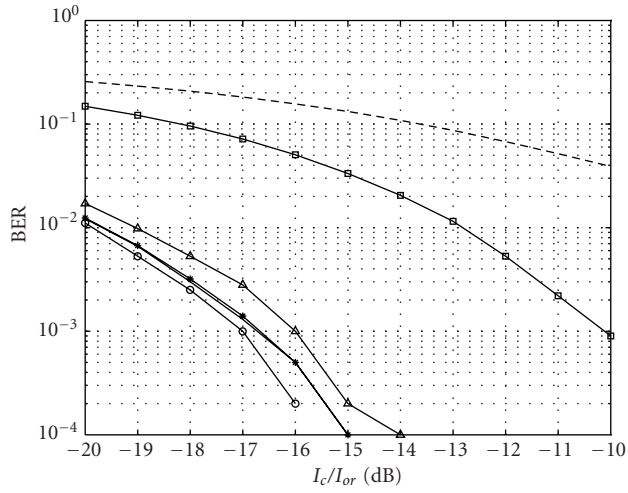

Figure 9: BER comparisons between rate-one STBC and beamforming with subspace tracking and quantized feedback schemes: $n_T = 4$ and $n_R = 1$; one QPSK symbol/transmission; $v = 3$ km/h; $(3, 6)$ quantized feedback.

Table 2: Summary of the performance comparisons of the MIMO techniques.

(a)

High-rate transmission	MIMO techniques	Channel information	BER performance
Four symbols/transmission over $n_T = 4$	BLAST	Receiver	Better
	Transmit precoding	Transmitter/receiver	Worse

(b)

Diversity transmission	MIMO techniques	channel Information	BER performance
One symbol/transmission over $n_T = 2$	Beamforming	Transmitter/receiver	Better
	Alamouti	Receiver	Worse
One symbol/transmission over $n_T = 4$	Beamforming	Transmitter/receiver	Better
	Rate-one STBC	Receiver	Worse
Two symbols/transmission over $n_T = 4$	Transmit precoding	Transmitter/receiver	Worse
	Rate-two STBC	Receiver	Better

the transmitter and the receiver; the second curve is the result of the beamforming scheme with perfectly known channel knowledge at the receiver and the frame-based feedback without quantization; the third curve is the result of the beamforming scheme with perfectly known channel knowledge at the receiver and the frame-based feedback with $(3, 6)$ quantization; the fourth curve is the result of channel estimator, subspace tracker, and the frame-based feedback with $(3, 6)$ quantization; the top two curves are the results of the rate-one STBC scheme with different detection methods. It is observed from Figure 9 that the beamforming can achieve a much better performance than the STBC for the case of four transmit antennas.

Moreover, it is also well confirmed that the subspace tracking algorithm discussed in Section 3.2.1, the frame-based feedback in Section 3.2.2, as well as the quantization approach discussed in Section 3.2.3 offer a practical way of realizing beamforming in MIMO WCDMA systems.

5. CONCLUSIONS

In this paper, we have analyzed and compared the performance of three MIMO techniques, namely, BLAST, STBC and linear precoding/decoding, and considered their applications in WCDMA downlink systems. For a certain transmission rate, we compared the different scenarios with different transmit antennas both analytically in terms of the average receiver SNR, as well as through simulations in terms of the BER performance. To cope with the channel feedback in WCDMA systems for beamforming, we adopted a subspace tracking method with a quantized feedback approach to make the principle eigenspace of the MIMO channel available to the transmitter.

Some instructive conclusions are drawn in this study. On the one hand, the optimal BLAST scheme can achieve the best performance in the high-rate transmission scenario, although with channel knowledge available at the transmitters, no performance gain is achievable by the linear precoding/decoding schemes without employing adaptive modulation. On the other hand, the beamforming scheme achieves better performances than the STBC schemes in the diversity transmission scenario. Table 2 gives a summary of the performance comparisons of the MIMO techniques in different scenarios. Moreover, it is well confirmed the effectiveness and feasibility of the combination of the subspace tracking algorithm and the quantized feedback approach for beamforming transmission in the MIMO WCDMA system. Finally, we note that in this paper, we only consider the *linear* precoding scheme. Significant performance improvement is expected when nonlinear precoder (e.g., adaptive modulation and bit loading) is employed [26, 27, 28].

ACKNOWLEDGMENT

This work was supported in part by the U.S. National Science Foundation (NSF) under Grants CCR-0225721 and CCR-0225826.

REFERENCES

[1] C.-N. Chuah, D. N. C. Tse, J. M. Kahn, and R. A. Valenzuela, "Capacity scaling in MIMO wireless systems under correlated fading," *IEEE Transactions on Information Theory*, vol. 48, no. 3, pp. 637–650, 2002.

[2] G. J. Foschini and M. J. Gans, "On limits of wireless communication in a fading environment when using multiple antennas," *Wireless Personal Communications*, vol. 6, no. 3, pp. 311–355, 1998.

[3] D.-S. Shiu, G. J. Foschini, M. J. Gans, and J. M. Kahn, "Fading correlation and its effect on the capacity of multielement antenna systems," *IEEE Trans. Communications*, vol. 48, no. 3, pp. 502–513, 2000.

[4] O. Damen, A. Chkeif, and J.-C. Belfiore, "Lattice code decoder for space-time codes," *IEEE Communications Letters*, vol. 4, no. 5, pp. 161–163, 2000.

[5] G. J. Foschini, "Layered space-time architecture for wireless communication in a fading environment when using multi-element antennas," *Bell Labs Tech. Journal*, vol. 1, no. 2, pp. 41–59, 1996.

[6] G. D. Golden, C. J. Foschini, R. A. Valenzuela, and P. W. Wolniansky, "Detection algorithm and initial laboratory results using V-BLAST space-time communication architecture," *Electronics Letters*, vol. 35, no. 1, pp. 14–16, 1999.
[7] H. Sampath, P. Stoica, and A. Paulraj, "Generalized linear precoder and decoder design for MIMO channels using the weighted MMSE criterion," *IEEE Transactions on Communications*, vol. 49, no. 12, pp. 2198–2206, 2001.
[8] S. M. Alamouti, "A simple transmit diversity technique for wireless communications," *IEEE Journal on Selected Areas in Communications*, vol. 16, no. 8, pp. 1451–1458, 1998.
[9] V. Tarokh, H. Jafarkhani, and A. R. Calderbank, "Space-time block codes from orthogonal designs," *IEEE Transactions on Information Theory*, vol. 45, no. 5, pp. 1456–1467, 1999.
[10] V. Tarokh, H. Jafarkhani, and A. R. Calderbank, "Space-time block coding for wireless communications: performance results," *IEEE Journal on Selected Areas in Communications*, vol. 17, no. 3, pp. 451–460, 1999.
[11] Z. Hong, K. Liu, R. W. Heath, and A. M. Sayeed Jr., "Spatial multiplexing in correlated fading via the virtual channel representation," *IEEE Journal on Selected Areas in Communications*, vol. 21, no. 5, pp. 856–866, 2003.
[12] L. Zheng and D. N. C. Tse, "Diversity and multiplexing: a fundamental tradeoff in multiple-antenna channels," *IEEE Transactions on Information Theory*, vol. 49, no. 5, pp. 1073–1096, 2003.
[13] K. Majonen and M. J. Heikkila, "Higher data rates with space-time block codes and puncturing in WCDMA systems," in *Proc. IEEE International Symposium on Personal, Indoor, and Mobile Radio Communications (PIMRC '01)*, pp. 36–40, San Diego, Calif, USA, October 2001.
[14] D. Samardzija, P. Wolniansky, and J. Ling, "Performance evaluation of the VBLAST algorithm in W-CDMA systems," in *IEEE Vehicular Technology Conference (VTC '01)*, vol. 2, pp. 723–727, Atlantic City, NJ, USA, October 2001.
[15] Texas Instruments, "Space-time block coded transmit antenna diversity for WCDMA," proposal TDOC# 662/98 to ETSI SMG2 UMTS standards, December 1998.
[16] Lucent Technologies, "Downlink diversity improvements through space-time spreading," proposal 3GPP2-C30-19990817-014 to the CDMA-2000 standard, August 1999.
[17] B. C. Banister and J. R. Zeidler, "Tracking performance of a gradient sign algorithm for transmit antenna adaptation with feedback," in *Proc. IEEE Int. Conf. Acoustics, Speech, Signal Processing (ICASSP '01)*, Salt Lake City, Utah, USA, May 2001.
[18] B. C. Banister and J. R. Zeidler, "Transmission subspace tracking for MIMO communications systems," in *Proc. IEEE Global Telecommunications Conference (GLOBECOM '01)*, vol. 1, pp. 161–165, San Antonio, Tex, USA, November 2001.
[19] W. Utschick, "Tracking of signal subspace projectors," *IEEE Transactions on Signal Processing*, vol. 50, no. 4, pp. 769–778, 2002.
[20] X. Wang and H. V. Poor, "Blind multiuser detection: a subspace approach," *IEEE Transactions on Information Theory*, vol. 44, no. 2, pp. 677–690, 1998.
[21] Third Generation Partnership Project, "Tx diversity solutions for multiple antennas (release 5)," proposal 3G TR25.869 V0.1.01 to Technical Specification Group Radio Access Network, November 2001.
[22] G. J. Foschini, G. D. Golden, R. A. Valenzuela, and P. W. Wolniansky, "Simplified processing for high spectral efficiency wireless communication employing multi-element arrays," *IEEE Journal on Selected Areas in Communications*, vol. 17, no. 11, pp. 1841–1852, 1999.
[23] B. Hochwald, T. L. Marzetta, and C. B. Papadias, "A transmitter diversity scheme for wideband CDMA based on space-time spreading," *IEEE Journal on Selected Areas in Communications*, vol. 19, no. 1, pp. 48–60, 2001.
[24] C. B. Papadias and G. J. Foschini, "A space-time coding approach for systems employing four transmit antennas," in *Proc. IEEE Int. Conf. Acoustics, Speech, Signal Processing (ICASSP '01)*, pp. 2481–2484, Salt Lake City, Utah, USA, May 2001.
[25] T. L. Marzetta, "Blast training: estimating channel characteristics for high capacity space-time wireless," in *Proc. 37th Annual Allerton Conference on Communication, Control, and Computing*, pp. 958–966, Monticello, Ill, USA, September 1999.
[26] P. S. Chow, J. M. Cioffi, and J. A. C. Bingham, "A practical discrete multitone transceiver loading algorithm for data transmission over spectrally shaped channels," *IEEE Trans. Communications*, vol. 43, no. 2, pp. 773–775, 1995.
[27] R. F. H. Fischer and J. B. Huber, "A new loading algorithm for discrete multitone transmission," in *Proc. IEEE Global Telecommunications Conference (GLOBECOM '96)*, pp. 724–728, London, England, November 1996.
[28] B. S. Krongold, K. Ramchandran, and D. L. Jones, "Computationally efficient optimal power allocation algorithms for multicarrier communication systems," *IEEE Trans. Communications*, vol. 48, no. 1, pp. 23–27, 2000.

Chuxiang Li received the B.S. and M.S. degrees from the Department of Electronics Engineering, Tsinghua University, Beijing, China, in 1999 and 2002, respectively. He is currently working toward the Ph.D. degree in the Department of Electrical Engineering, Columbia University, New York, NY. His research interests fall in the area of wireless communications and statistical signal processing.

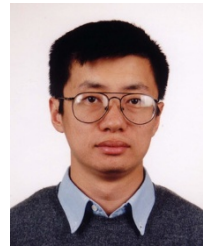

Xiaodong Wang received the B.S. degree in electrical engineering and applied mathematics (with the highest honor) from Shanghai Jiao Tong University, Shanghai, China, in 1992; the M.S. degree in electrical and computer engineering from Purdue University in 1995; and the Ph.D. degree in electrical engineering from Princeton University in 1998. From July 1998 to December 2001, he was an Assistant Professor in the Department of Electrical Engineering, Texas A&M University. In January 2002, he joined the Department of Electrical Engineering, Columbia University, as an Assistant Professor. Dr. Wang's research interests fall in the general areas of computing, signal processing, and communications. He has worked in the areas of digital communications, digital signal processing, parallel and distributed computing, nanoelectronics, and bioinformatics, and has published extensively in these areas. His current research interests include wireless communications, Monte-Carlo-based statistical signal processing, and genomic signal processing. Dr. Wang received the 1999 National Science Foundation (NSF) Career Award, and the 2001 IEEE Communications Society and Information Theory Society Joint Paper Award. He currently serves as an Associate Editor for the IEEE Transactions on Communications, the IEEE Transactions on Wireless Communications, the IEEE Transactions on Signal Processing, and the IEEE Transactions on Information Theory.